RESEARCH ARTICLE

Polysaccharide hydrolysis in the presence of oil and dispersants: Insights into potential degradation pathways of exopolymeric substances (EPS) from oil-degrading bacteria

Kai Ziervogel[*], Samantha B. Joye[†], Sara Kleindienst[‡], Sairah Y. Malkin[§], Uta Passow[∥], Andrew D. Steen[¶] and Carol Arnosti[**]

Oceanic oil-degrading bacteria produce copious amounts of exopolymeric substances (EPS) that facilitate their access to oil. The fate of EPS in the water column is in part determined by activities of heterotrophic microbes capable of utilizing EPS compounds as carbon and energy sources. To evaluate the potential of natural microbial communities to degrade EPS produced during oil degradation, we measured potential hydrolysis rates of six structurally distinct polysaccharides in two roller bottle experiments, using water from a natural oil seep in the northern Gulf of Mexico. The suite of polysaccharides used to measure the initial step in carbon degradation is indicative of polymers within microbial EPS. The treatments included (i) unamended surface or deep waters (whole water), and water amended with (ii) a water-accommodated fraction of oil (WAF), (iii) oil dispersant Corexit 9500, and (iv) WAF chemically-enhanced with Corexit (CEWAF). The oil and Corexit treatments were employed to simulate conditions during the Deepwater Horizon oil spill. Polysaccharide hydrolysis rates in the surface-water treatments were lowest in the WAF treatment, despite elevated levels of EPS in the form of transparent exopolymer particles (TEP). In contrast, the three deep-water treatments (WAF, Corexit, CEWAF) showed enhanced hydrolysis rates and TEP levels (WAF) compared to the whole water. We also observed variations in the spectrum of polysaccharide-hydrolyzing enzyme activities among the treatments. These substrate specificities were likely driven by activities of oil-degrading bacteria, shaping the pool of EPS and TEP as well as degradation products of hydrocarbons and Corexit compounds. A model calculation of potential turnover rates of organic carbon within the TEP pool suggests extended residence times of TEP in oil-contaminated waters, making them prone to serve as the sticky matrix for oily aggregates known as marine oil snow.

1. Introduction

Oil degradation facilitated by specialized microbial communities plays a key role in the fate of petroleum hydrocarbons in the ocean (Head et al., 2006). A hotspot of indigenous oil-degrading bacteria is the northern Gulf of Mexico, where at least 914 natural hydrocarbon seep zones, overlying subseafloor oil reservoirs, discharge oil into the water column at an annual rate of $2.5–9.4 \times 10^4$ $m^3 \, yr^{-1}$ (MacDonald et al., 2015). Natural oil and gas seeps promote growth of microbial populations equipped to metabolize low to moderate levels of hydrocarbons and gas (Joye et al., 2010). During the Deepwater Horizon spill in 2010, however, the volume of oil discharged into the northern Gulf of Mexico ($\sim500 \times 10^3$ m^3 over 5 months) overshadowed natural input levels.

The Deepwater Horizon discharge was the first oil-industry accident of this magnitude that affected deep-sea environments: massive quantities of oil and gas were released from the broken riser pipe, forming hydrocarbon plumes at depths between 1000 m and 1300 m (Diercks et al., 2010). Deep-water oil and gas plumes selected for highly active bacterial oil-degrading communities of a composition quite distinct from that found in non-plume deep waters (Hazen et al., 2010; Valentine et al.,

[*] University of New Hampshire, Durham, New Hampshire, US

[†] University of Georgia, Athens, Georgia, US

[‡] University of Tuebingen, Tuebingen, DE

[§] University of Maryland, Cambridge, Maryland, US

[∥] Memorial University of Newfoundland, St. John's, CA

[¶] University of Tennessee, Knoxville, Tennessee, US

[**] University of North Carolina, Chapel Hill, North Carolina, US

Corresponding author: Kai Ziervogel (kai.ziervogel@unh.edu)

2010; Redmond and Valentine, 2011; Kleindienst et al., 2016) and oil-contaminated surface waters (Yang et al., 2016). In both the deep-water plumes and surface waters impacted by the oil spill, copious amounts of exoplymeric substances (EPS), produced and excreted by oil-degrading bacteria to emulsify petroleum hydrocarbons (Gutierrez et al., 2013), formed mucus-like particles or flocs (Bælum et al., 2012; Passow et al., 2012) that acted as "glue" for oily aggregates (marine oil snow), accelerating sedimentation of spilled oil across a large area (Chanton et al., 2015; Passow and Ziervogel, 2016).

EPS from oil degradation are comprised mainly of polysaccharides, proteins, and lipids (Quigg et al., 2016), and these labile substrates stimulate the activities of heterotrophic secondary consumers not directly associated with oil degradation (Head et al., 2006). During the spill, rates of organic matter degradation by heterotrophic microbes were higher in oil-contaminated surface (Edwards et al., 2011; Ziervogel et al., 2012; Arnosti et al., 2016) and deep waters (Ziervogel and Arnosti, 2016) relative to uncontaminated waters, suggesting a potential interaction between organic matter and EPS from oil degradation and bacterial secondary consumers.

Interactions within bacterial oil-degradation cascades during the 2010 oil spill were affected by the extensive application of chemical dispersants (~7 × 10^6 L of mainly Corexit 9500; Kujawinski et al., 2011), which were injected directly at the discharging wellhead and applied onto surface slicks to increase the solubility of oil. While the effectiveness of Corexit with respect to oil bioremediation remains unclear, dispersants shaped bacterial community compositions during the 2010 spill (Kleindienst et al., 2015a, and references therein). Mesocosm experiments with Gulf of Mexico bacterial communities indicated that Corexit compounds may act as an additional carbon source for heterotrophic bacteria, selecting for specific oil-degrading populations that were distinct from those not amended with Corexit (Bælum et al., 2012; Kleindienst et al., 2015b; Techtmann et al., 2017). Biodegradation of Corexit compounds and dispersed oil affects the composition of oil-degradation byproducts (Seidel et al., 2016) available to bacterial secondary consumers within oil-degradation cascades. Moreover, Corexit may change the quantity and composition of EPS (van Eenennaam et al., 2016; Xu et al., 2018), with possible consequences for heterotrophic microbial activities and food web interactions in the case of an oil spill.

To better understand the initial transformation step of oil-degradation byproducts including EPS derived from oil degraders, we measured potential hydrolysis rates of high molecular weight organic matter (polysaccharides) by indigenous bacterial populations from the Gulf of Mexico exposed to oil under Deepwater Horizon-like conditions. The main goal of this study was to investigate whether oil contamination leads to enhanced polysaccharide degradation by natural microbial assemblages.

Our data set was generated during two separate laboratory experiments designed to assess the effects of oil and Corexit exposure on natural bacterial communities from surface and deep waters collected near a natural oil seep in the northern Gulf of Mexico (Kleindienst et al., 2015b; Malkin et al., 2019). The sampling site over the Green Canyon (GC) oil reservoir is located approximately 322 km (200 miles) off the Louisiana coast. The site is characterized by comparatively low rates of primary productivity and POC fluxes to depth relative to the Deepwater Horizon oil spill site, which is located in the Mississippi Canyon near the main Mississippi River Delta (Giering et al., 2018).

Polysaccharides were chosen as substrates for microbial enzymatic activities as they often comprise a major fraction of EPS from oil-degrading bacteria (Gutierrez et al., 2013). The six polysaccharides used here — arabinogalactan, chondroitin sulfate, fucoidan, laminarin, pullulan, and xylan — differ in monomer composition and linkage position; many are present in considerable quantities in the ocean (Alderkamp et al., 2007). Enzymes that specifically hydrolyze these substrates have been identified in a variety of marine environments (Arnosti et al., 2011) as well as in the genomes of recently sequenced marine bacterial isolates (Glöckner et al., 2003; Bauer et al., 2006; Weiner et al., 2008). Moreover, most of the structural monosaccharides of the six polysaccharides used here were found in the EPS pool from Gulf of Mexico surface-water microbial assemblages experimentally exposed to oil and Corexit (Xu et al., 2018), and from bacteria isolates associated with oil slicks from the 2010 Gulf of Mexico spill (Gutierrez et al., 2018).

Polysaccharide hydrolysis rates were measured in the following treatments of the two mesocosm experiments: whole water (either surface or deep water from a natural oil seep in the northern Gulf of Mexico) amended with: (i) a water-accommodated fraction of crude oil (WAF); (ii) WAF chemically enhanced with Corexit (CEWAF); (iii) Corexit only; and (iv) unamended whole water. WAF and CEWAF are commonly used to study toxicity effects of petroleum hydrocarbons under controlled laboratory conditions (e.g., Wade et al., 2017). Polysaccharide hydrolysis patterns were compared with bacterial cell numbers and transparent exopolymer particles (TEP), a particulate form of EPS (Passow, 2002), to estimate turnover rates by microbial communities in the Gulf of Mexico.

2. Material and Methods
2.1. Mesocosm set-up
This study was part of two distinct laboratory mesocosm experiments using seawater collected at a site with active natural hydrocarbon seepage (GC600; 27° 21.79′N, 90° 34.65′W). The first incubation (hereafter referred to as deep-water experiment) was prepared with GC 600 bottom water sampled at a depth of 1178 m in March 2013 using Niskin bottles attached to a CTD rosette during RV *Pelican* cruise 13–21. The second incubation (hereafter referred to as surface-water experiment) was conducted with GC 600 surface water collected during RV *Pelican* cruise 15-08 in September 2014. Surface-water samples were collected with a clean bucket that was lowered repeatedly from the deck into a surface oil slick.

A detailed description of sample storage and preparation of the incubations, as well as a complete description

of the parameters analyzed, is given for the deep-water experiment in Kleindienst et al. (2015b) and for the surface-water experiment in Malkin et al. (2019). In brief, individual surface- and deep-water incubations were prepared with unamended source water (whole water) and with whole water prepared using three distinct treatments: (i) with a water-accommodated fraction of Macondo oil (WAF); (ii) with a mixture of Corexit 9500 and WAF yielding CEWAF; and (iii) with the dispersant agent Corexit 9500 (Corexit-only) (**Table S1**). WAF represents the fraction of crude oil that dissolves into the aqueous phase, and is comprised mainly of lower molecular weight aromatic hydrocarbons (Overton et al., 2016; Wade et al., 2017). The addition of Corexit changes the surface area of oil, potentially increasing the biodegradability of oil (Kleindienst et al., 2015a). The WAF used for our mesocosm experiments contained concentrations of total petroleum hydrocarbons similar to those observed in the water column during the 2010 spill (Kleindienst et al., 2015b). Concentrations of Corexit were also comparable to those in the deep-water plumes during the spill (Kleindienst et al., 2015b).

All treatments were incubated in triplicate 2-L glass bottles in the dark on a roller table at 15 rpm, which ensured incubation under mildly turbulent conditions. Incubation temperatures were close to the respective in situ temperatures at the time of sampling (surface water: 23°C; deep water: 7°C); incubation times varied between 8 days (surface-water experiment; i.e., short experiment in Malkin et al., 2019) and 6 weeks (deep-water experiment).

2.2. Polysaccharide hydrolysis

Rates of polysaccharide hydrolysis were measured in the whole water before the start of the roller table incubation (hereafter referred to as initial whole water), and in the whole water and WAF-, Corexit-, and CEWAF-amended roller bottles sampled at the end of the roller table incubations. Note that samples from intermediate time points as described in Kleindienst et al. (2015b) and Malkin et al. (2019) were not available for this study due to limited volumes available for experimentation.

Six polysaccharides — arabinogalactan, chondroitin sulfate, fucoidan, laminarin, pullulan, and xylan (all Sigma or Fluka; **Table 1**) — were labeled with fluoresceinamine and used as substrate for extracellular

enzymes as described in Arnosti (1996, 2003). In brief, single substrates were added to pre-autoclaved 17-mL glass vials at a final concentration of 3.5 μM monomer equivalent. Five mL from each roller bottle were added to the vials containing single substrates. Incubations from the surface-water experiment were conducted with triplicate vials per substrate and treatment; two replicate vials per substrate and treatment were prepared for the deep-water experiment. Fewer replicates were made for the deep-water experiment due to the limited quantity of water available. Because of the need for adequate sample volume, we had to pool the subsamples from each replicate roller bottle and divide them into 5-mL portions for each of the six substrates.

Enzymatic hydrolysis of single substrates was monitored over time (total incubation time: 22 days) by means of gel-permeation chromatography (GPC) as described in detail in Arnosti (2003). In brief, samples were injected onto a GPC system consisting of a Shimadzu LC-10 AT HPLC pump connected in series to a G-50 Sephadex gel column (20.5 × 1 cm) and a G-75 Sephadex gel column (18 × 1 cm), with the column outflow passing to a Hitachi fluorescence detector L-2480 set to excitation and emission maxima of 490 and 530 nm, respectively. The mobile phase was 100 mM NaCl + 50 mM Na_2HPO_4/NaH_2PO_4 phosphate buffer (pH 8.0) at 1 ml min^{-1} flow rate. The column set was calibrated with a series of FITC dextran standards (150 kD, 10 kD, 4 kD, FITC galactose, and free fluorescent tag, all obtained from Sigma) in order to determine the elution time corresponding to different molecular weight size classes.

Throughout the 22-day incubations, the incubation vials were kept static in the dark, and at the respective *in situ* temperatures. One mL subsample was removed from each of the incubation vials after 0, 3, 7, 14, 22 days and filtered through 0.2-μm syringe filters. The filtrate was stored at –20°C until analysis on the GPC system. The polysaccharide hydrolysis incubation time points are separate and differ from the mesocosm time points.

Polysaccharide hydrolysis incubations, as in this study, are conducted as a time series over periods of days to weeks, because the time that is required for a polysaccharide pool to be hydrolyzed to lower molecular weights is not known *a priori*. Hydrolysis rates for each of the four

Table 1: Chemical description of polysaccharides used for hydrolysis experiments. DOI: https://doi.org/10.1525/elementa.371.t1

Substrate	Description	MW (kD)[a]
Arabinogalactan	mixed polymer of galactose and arabinose	~72–92
Chondroitin sulfate	sulfated polymer of N-acetylgalactosamine and glucuronic acid	63
Fucoidan	Fucose-containing sulfated polysaccharide	~100
Laminarin	β(1,3)-linked glucose polymer	8.6
Pullulan	α(1,6)-linked maltotriose polymer	71.5
Xylan	β(1,4)-linked xylose	8

[a] Molecular weights (MW) according to Sigma.

time points were calculated from the changes of high molecular weight substrates to lower molecular weight products as a result of enzymatic hydrolysis; these rates were corrected for any hydrolysis in killed control water (0.2 μm-filtered and pasteurized for 2 h at 65°C). The maximum hydrolysis rate among all time points in a sample was used as a measure of the maximum potential rate at which the microbial community could access a specific polysaccharide. The sum of the maximum hydrolysis rates for each substrate (hereafter referred to as summed hydrolysis rate) was used to illustrate the overall hydrolytic potential of the heterotrophic communities for polysaccharide degradation.

The rates reported here represent potential hydrolysis rates, as added substrate competes with naturally occurring substrates for active enzyme sites. Given the level of substrate addition, however, hydrolysis rates are likely zero order with respect to substrate and represent maximum potential rates.

2.3. Bacterial cell counts and transparent exopolymer particles (TEP)

Sample preparation and analysis of bacterial cell counts and transparent exopolymer particles (TEP) are described in Kleindienst et al. (2015b) and Malkin et al. (2019). In brief, microbial cell counts were conducted using epifluorescence microscopy after staining the cells with either SYBR Gold (ThermoFisher; surface-water experiment) or 4′,6-Diamidino-2-phenylindole (DAPI, Sigma; deep-water experiment).

TEP are a particulate form of microbial EPS that play an important role in microbe-oil interactions and the formation of marine oil snow (Passow et al., 2017). TEP were measured colorimetrically using the Alcian Blue method (Passow and Alldredge, 1995) with Xanthan Gum (Sigma) as a standard solution, and TEP concentrations are reported as Xanthan Gum equivalents per unit water volume (XG eq. L⁻¹). TEP could not be analyzed in roller bottles that contained Corexit due to chemical interference of the Corexit with Alcian Blue. The carbon content of TEP (TEP-C; μg C L⁻¹) was calculated using the concentration-dependent relationship between POC and TEP proposed by Engel and Passow (2001). Cell counts and TEP concentrations, previously reported for the deep-water experiment in Kleindienst et al. (2015b) and for the

surface-water experiment in Malkin et al. (2019), are used here for the interpretation of our results on polysaccharide hydrolysis patterns.

2.4. TEP-C turnover rates

To estimate the fate of oil-derived EPS within the TEP pool, we calculated TEP-C turnover per day as the ratio of C remineralization rates (μg C L⁻¹ d⁻¹) to TEP-C (μg C L⁻¹) in the whole water and WAF treatments. Carbon remineralization rates were calculated from summed polysaccharide hydrolysis in the respective treatments, assuming 6 C remineralized per hydrolyzed monomer. For this model calculation, we assumed that hydrolysis rates of the six polysaccharides tested here are representative of all EPS hydrolysis in the treatments. We also assumed that all EPS produced during microbial oil degradation partitioned into the TEP pool.

2.5. Statistical analysis

The uncertainties of the summed maximum hydrolysis rates are assumed by the error propagation of the individual standard deviations given by

$$\sigma_y = \frac{1}{N} \sqrt{\sigma_a^2 + \sigma_b^2 + \ldots + \sigma_n^2}$$

where σ_a is the standard deviation of the hydrolysis rate of the first substrate, σ_b is the standard deviation of the second substrate, and N is the number of replicates. ANOVA, PERMANOVA and PCA were performed using the R language and the vegan version 2.4-5 on standardized data, which analyzed the change in patterns of hydrolysis rates without respect to changes in summed hydrolysis rates (Oksanen et al., 2017). Student's t-test was performed using JMP Pro 14 software.

3. Results

Table 2 illustrates selected ancillary data on the initial (unamended) surface and deep water at the time of sampling (see Kleindienst et al., 2015b, and Malkin et al., 2019, for more details). DOC levels at the surface were about double those at 1178 m, and inorganic nutrients were an order of magnitude lower (or undetectable in the case of SRP) at the surface compared to the deep-water sample.

Table 2: Ancillary data on the unamended water at the time of sampling and at initiation of the roller bottle experiments. DOI: https://doi.org/10.1525/elementa.371.t2

Sample[a]	Depth (m)	Salinity	T (°C)	Roller bottles[b]			
				DOC (μM)	SRP (μM)	NH₄ (μM)	NOx (μM)
Surfacewater	0[c]	36	23	96.9 ± 5.5	n.d.[d]	0.01 ± 0.01	0.3 ± 0.1
Deep water	1178	36	7	45.5 ± 5.4	1.7 ± 0.03	0.2 ± 0.1	24 ± 0.2

[a] Surface-water data from Malkin et al. (2019); deep-water data from Kleindienst et al. (2015b).
[b] DOC indicates dissolved organic carbon; SRP, soluble reactive phosphorus; NOx, nitrate + nitrite; WAF, water accommodated fraction of oil; CEWAF, chemically enhanced (with Corexit) WAF. Values ± standard deviation, n = 3 replicate bottles.
[c] Water samples taken by bucket from the sea surface.
[d] Not detectable.

3.1. Polysaccharide hydrolysis in surface-water roller bottles

The oil and Corexit treatments significantly influenced the summed hydrolysis rates (ANOVA, $p < 0.01$; **Figure 1A**). The initial whole water and whole water roller bottles showed very similar summed hydrolysis rates, indicating that the roller table incubation time and conditions had only minor effects on overall hydrolytic activities in the two unamended treatments. Summed hydrolysis rates in the CEWAF treatment were also similar to the initial whole water sample. Summed hydrolysis rates in the Corexit-only treatment were 73% of the rates in the initial whole water, which was not distinguishable statistically based on the experimental design used here ($p > 0.05$; Tukey's HSD post-hoc test). Summed hydrolysis rates in the WAF treatment were 58% of the initial whole water rates, which was distinguishable statistically ($p < 0.05$) from all treatments except the Corexit-only treatment.
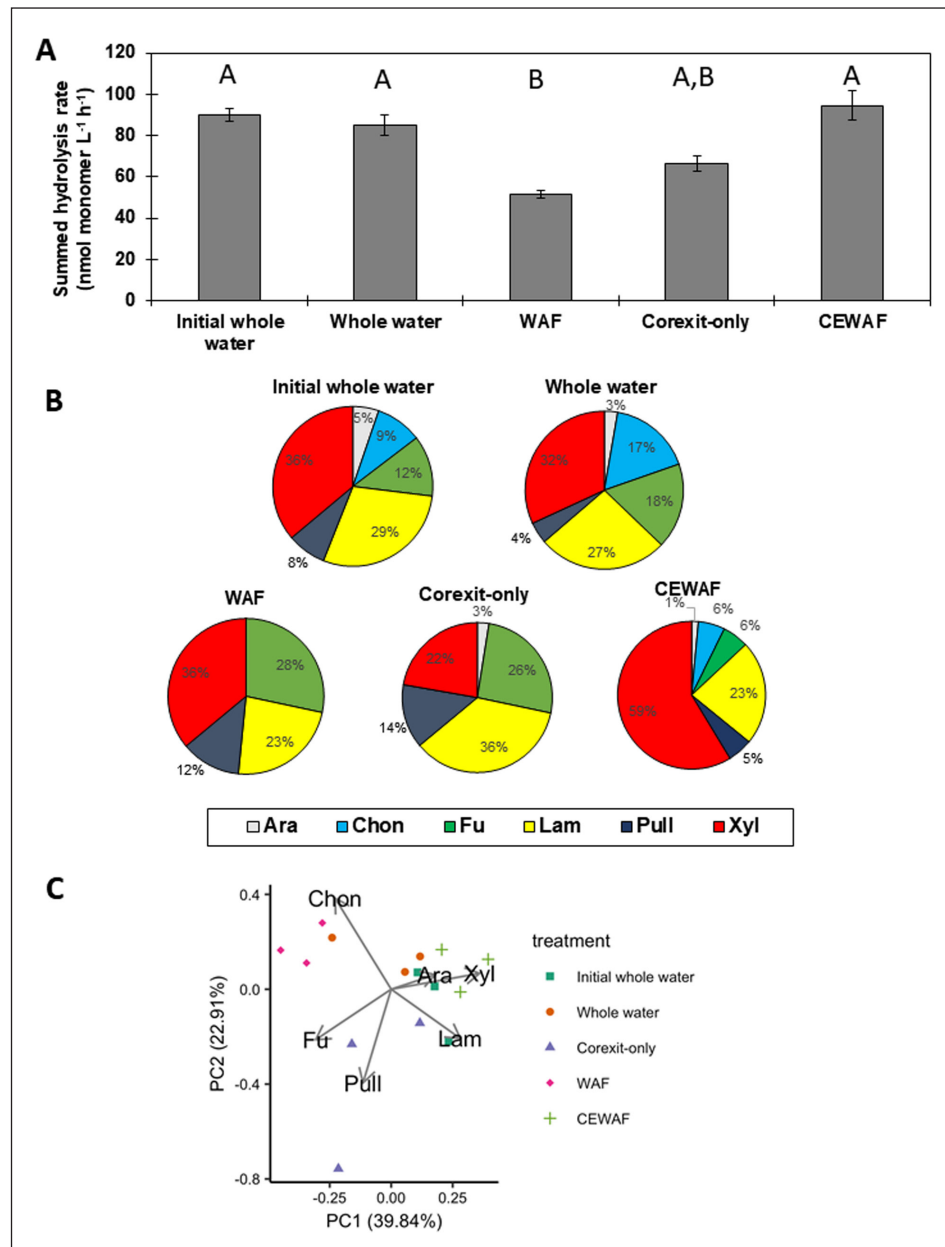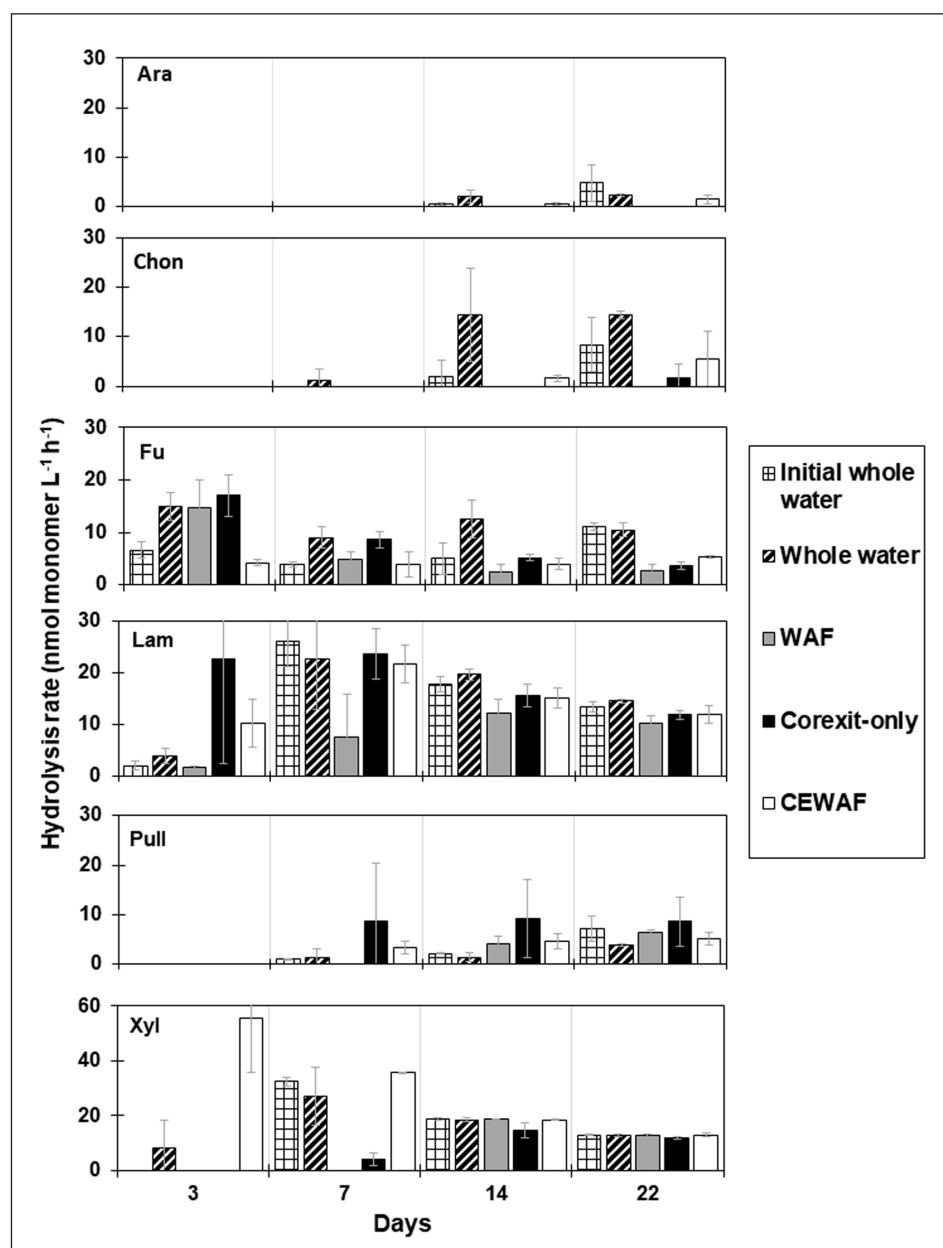

Figure 1: Polysaccharide hydrolysis in surface-water roller bottles. (A) Summed hydrolysis rates in the surface-water roller bottles sampled prior to (Initial whole water) and at the end of the 8-day roller table incubation (Whole water, WAF, Corexit-only, CEWAF) (n = 18). Error bars indicate the error propagation of the individual hydrolysis rates. Letters indicate results of the post-hoc analysis of treatment-specific differences in rates (ANOVA, $p < 0.05$); rates with the same letters are indistinguishable from one another. **(B)** Relative contributions of arabinogalactan (Ara), chondroitin (Chon), fucoidan (Fu), laminarin (Lam), pullulan (Pull), and xylan (Xyl) hydrolysis to summed hydrolysis rates (n = 3). **(C)** Principle component analysis (PCA) of standardized hydrolysis rates. Points represent patterns of hydrolysis rates in individual samples, and arrows represent PCA loadings, i.e., the effect that hydrolysis rates of each substrate have on the position of a sample in the PCA plot. DOI: https://doi.org/10.1525/elementa.371.f1

Oil and corexit amendments also significantly influenced the pattern of hydrolysis rates (PERMANOVA; $p < 0.001$). Differences in summed hydrolysis rates were driven mainly by the spectrum of polysaccharide hydrolase activities. All six substrates were hydrolyzed in the two whole water incubations and the CEWAF amendment (**Figure 1B**). In the Corexit-only amendment, five of the six substrates (all but arabinogalactan) were hydrolyzed; chondroitin sulfate was hydrolyzed in only one of the replicate vials and at the last time point (**Figure 2**). The WAF treatment had the narrowest spectrum of enzyme activities; neither arabinogalactan nor chondroitin sulfate were hydrolyzed during the course of the incubation.

Rates of hydrolysis varied strongly by substrate. Xylan hydrolysis contributed substantially to the summed hydrolysis rates in surface-water roller bottles, ranging between 22% (Corexit-only) and 59% (CEWAF) of the total summed rate (**Figure 1B**). Laminarin hydrolysis was considerable in all treatments (23–36%). Fucoidan hydrolysis also contributed notably, with highest contributions in the WAF (28%) and Corexit-only (26%) treatments, followed by the two whole water treatments (12% and 18%) and the CEWAF (6%) amendment. Pullulan was hydrolyzed in all treatments, but at generally low rates; chondroitin sulfate and arabinogalactan hydrolysis was also detectable but only at low rates (generally less than 10% to the total summed rate) in some of the incubations.

PCA analysis indicates that, in surface waters, relative arabinogalactan and xylan hydrolysis rates were closely correlated, and were generally anticorrelated

Figure 2: Polysaccharide hydrolysis rates per time point in surface-water roller bottles. Time courses of arabinogalactan (Ara), chondroitin (Chon), fucoidan (Fu), laminarin (Lam), pullulan (Pull), and xylan (Xyl) hydrolysis in the surface-water roller bottles. Error bars are standard deviations of triplicates. Note the different scale of the y-axis for Xyl. DOI: https://doi.org/10.1525/elementa.371.f2

with relative fucoidan and pullulan hydrolysis rates (**Figure 1C**). Relative chondroitin and laminarin hydrolysis rates were anticorrelated with each other. The pattern in the WAF treatment was driven by relatively rapid chondroitin hydrolysis and low xylan and arabinogalactan hydrolysis. The hydrolysis pattern in the CEWAF treatment was driven by rapid xylan and arabinogalactan hydrolysis, while the Corexit-only treatment was driven by relatively rapid pullulan and fucoidan hydrolysis and slow arabinogalactan, xylan, and chondroitin hydrolysis.

The time course of hydrolysis – and the time point when maximum hydrolysis rates of individual substrates were found – differed substantially among the surface-water treatments. For instance, xylan hydrolysis peaked in the CEWAF treatment at the initial time point of day 3 (**Figure 2** and **Table 3**); in the two whole water treatments, maximum xylan hydrolysis was found at day 7, while rates in the Corexit-only and WAF amendment were highest at day 14 of the hydrolysis incubation. Most rapid fucoidan hydrolysis was found in the whole water, WAF, and Corexit-only treatment at day 3, while maximum fucoidanase activity in the initial whole water and CEWAF were found only at the last time point (day 22).

3.2. Polysaccharide hydrolysis in deep-water roller bottles

Summed hydrolysis rates in the two unamended deep-water treatments were comparable to one another but were only about half the level measured in the three amended treatments (**Figure 3A**). These differences were not statistically distinguishable from one another (ANOVA, $p > 0.05$), due in part to the low statistical power of the experimental design. As in the surface-water samples, however, the relative contributions to summed activities varied by substrate and treatment (PERMANOVA, $p < 0.002$; **Figure 3B**). The effect that each treatment had on hydrolysis rate differed from that in the surface incubations.

In deep incubations, chondroitin sulfate contributed substantially to summed hydrolysis rates in all treatments (17–43%) and was particularly elevated in the initial whole water, WAF and CEWAF treatments (**Figure 3B**).

The contribution of xylan hydrolysis was lower in the WAF (19%) and the initial whole water (17%) compared to the other three treatments (34–47%). Relative contributions of xylan hydrolysis in the deep-water treatments were generally lower compared to those in the surface-water experiment. Laminarinase activities were comparable among the deep-water treatments (28–37%) except for CEWAF, adding only 19% of the total. Pullulan hydrolysis was overall lowest reaching 4% of the summed hydrolysis rates in the amended treatments, as well as 6% and 13% in the two unamended treatments. Both laminarin and pullulan hydrolysis revealed very similar proportional contributions to summed rates in the deep-water and surface-water treatments. Unlike in surface incubations, arabinogalactan and fucoidan hydrolysis rates were zero in all deep-water treatments.

In deep waters, relative pullulan and chondroitin hydrolysis rates were anticorrelated, and relative laminarin and xylan hydrolysis rates were correlated to each other but largely orthogonal to pullulan and laminarin (**Figure 3C**).

The time courses of hydrolysis revealed some differences among the deep-water treatments. For instance, chondroitin sulfate hydrolysis was more rapid in the WAF and CEWAF amendments (peak at day 7; **Figure 4** and **Table 3**) compared to the Corexit treatment that reached highest rates at day 14. Maximum chondroitin sulfate hydrolysis in the two unamended whole water treatments were measured at day 22. Xylan hydrolysis was most rapid in the Corexit-only treatment (peak at day 3), followed by CEWAF (day 7), the two whole water treatments (day 7), and WAF (day 22).

3.3. Bacterial abundance and TEP

For the surface-water experiment, bacterial cell counts in the whole water treatment were comparable to the initial whole water (**Table 4**). Highest cell densities were found in the CEWAF treatment where they were almost double those in the whole water. Cell abundance in the WAF treatment was almost one order of magnitude lower than in the CEWAF treatment, while cell densities in the Corexit-only treatment were in the same range as those in the whole water.

Table 3: Significant treatment-specific differences in maximum hydrolysis rates by analysis of variance (ANOVA, p-values < 0.05), where letters[a] indicate results of the post-hoc analysis. DOI: https://doi.org/10.1525/elementa.371.t3

Treatment	Surface-water roller bottles[b]			Deep-water roller bottles[c]		
	Chon (0.03)	Fu (0.009)	Xyl (0.005)	Chon (0.001)	Lam (0.02)	Xyl (0.03)
initial whole water	AB[c]	A	AB	B	AB	B
whole water	A	A	B	B	B	AB
WAF	—[d]	A	B	A	A	AB
Corexit	AB	A	B	B	A	A
CEWAF	B	B	A	A	AB	AB

[a] Rates with the same letters are indistinguishable from one another.
[b] Differences were not significant for Ara, Lam and Pull (p-values of 0.25, 0.1, and 0.5, respectively).
[c] The p-value for Pull was 0.7; Ara and Fu were not hydrolyzed in the deep-water incubations.
[d] Chon remained unhydrolyzed in the WAF treatment.
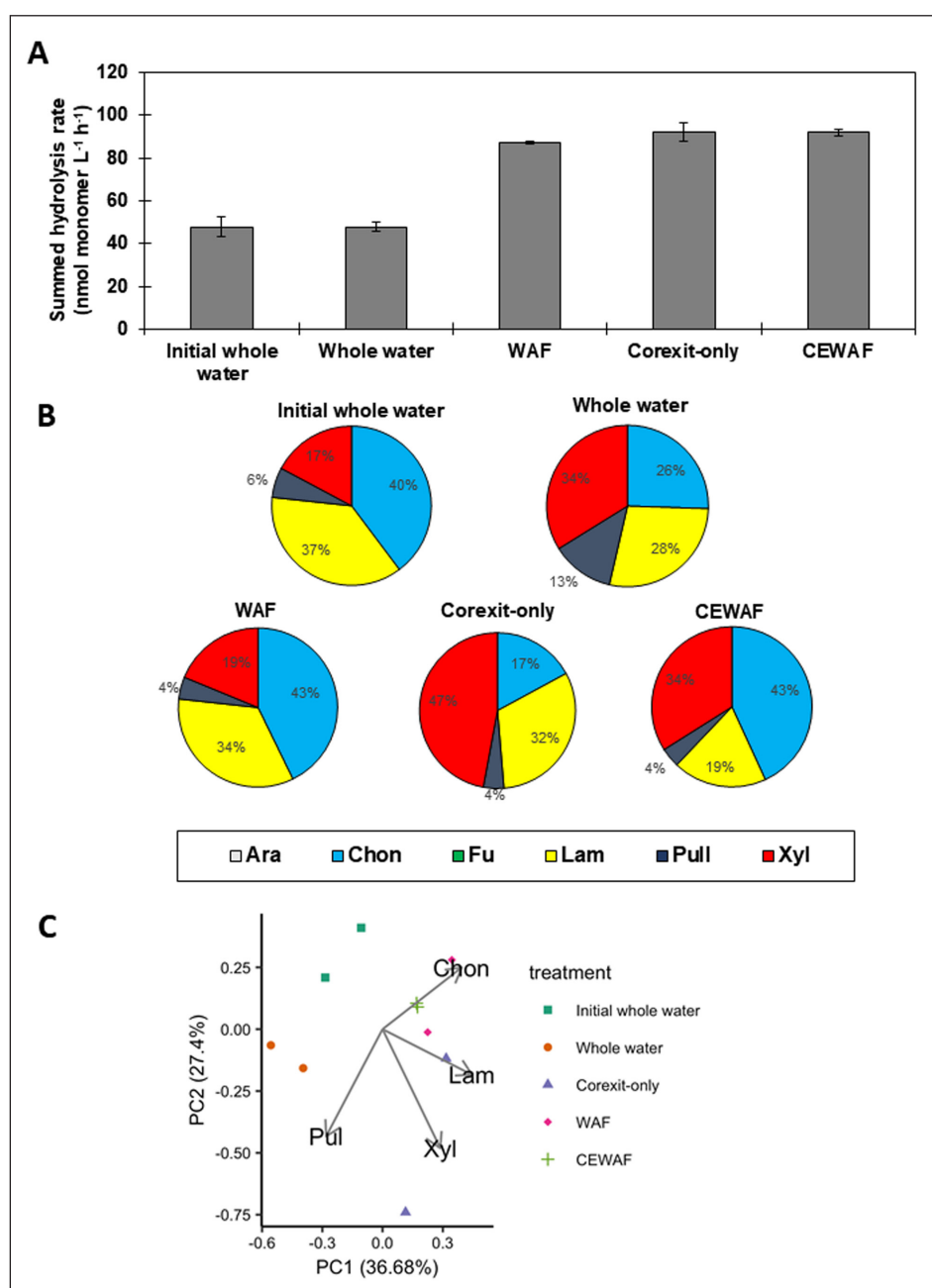
Figure 3: Polysaccharide hydrolysis in deep-water roller bottles. (A) Summed hydrolysis rates in the deep-water roller bottles sampled prior to (Initial whole water) and at the end of the 42-day roller table incubation (Whole water, WAF, Corexit-only, CEWAF) (n = 12). Error bars indicate the error propagation of the individual hydrolysis rates. Summed rates were not distinguishable statistically from one another (ANOVA, $p > 0.05$). **(B)** Relative contributions of chondroitin (Chon), laminarin (Lam), pullulan (Pull), and xylan (Xyl) hydrolysis to summed hydrolysis rates (n = 2). Note that arabinogalactan and fucoidan remained unhydrolyzed in the deep-water treatments. **(C)** Principle component analysis (PCA) of standardized hydrolysis rates. Points represent patterns of hydrolysis rates in individual samples, and arrows represent PCA loadings, i.e., the effect that hydrolysis rates of each substrate have on the position of a sample in the PCA plot. Note that arabinogalactan and fucoidan hydrolysis rates were zero in all treatments, and so were excluded from this analysis. DOI: https://doi.org/10.1525/elementa.371.f3

Average TEP concentration was highest in the WAF treatment, followed by the whole water and initial whole water. These differences were not statistically distinguishable from one another (ANOVA, $p > 0.05$).

In the deep-water roller bottles, highest cell numbers were found in the WAF treatment, followed by the Corexit-only treatment. Bacterial cell counts in the two unamended whole water treatments and the CEWAF were in the same range.

TEP levels in the two unamended deep whole water treatments were in the same range, and about half those in the deep WAF treatment. Average TEP-C turnover rates in the surface-water treatments were three times higher in the unamended water compared with WAF (**Figure 5**). These differences were not distinguishable statistically (t-test, $p = 0.1$) due to the high variance in whole water rates. In the deep water, TEP-C turnover was about 20 times higher in the unamended water compared to the WAF treatment (t-test, $p < 0.05$).
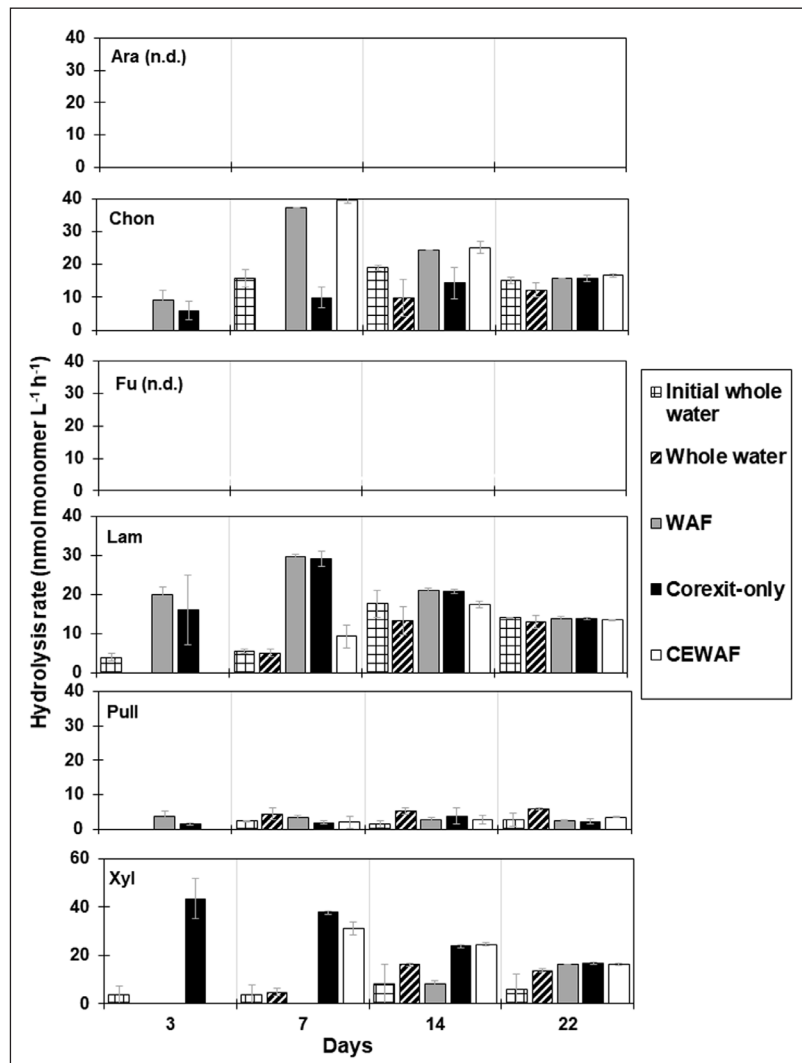
Figure 4: Polysaccharide hydrolysis rates per time point in deep-water roller bottles. Time courses of arabinogalactan (Ara), chondroitin (Chon), fucoidan (Fu), laminarin (Lam), pullulan (Pull), and xylan (Xyl) hydrolysis in the deep-water roller bottles. Error bars are standard deviations of replicate incubations (n = 2). Note the different scale of the y-axis for Xyl, and that hydrolysis of Ara and Fu was not detectable (n.d.). DOI: https://doi.org/10.1525/elementa.371.f4

Table 4: Bacterial abundance and TEP in surface- and deep-water roller bottles at the end of the experiments. DOI: https://doi.org/10.1525/elementa.371.t4

Sample[a]	Treatment	Bacterial cells (mL^{-1})	TEP (µg GX eq. L^{-1})	TEP-C (µg C L^{-1})
Surface water	initial whole water	$3.2 \times 10^4 \pm 4.9 \times 10^3$, AB[b]	85 ± 7	64 ± 5
	whole water	$2.8 \times 10^4 \pm 1.6 \times 10^4$, AB	154 ± 66	116 ± 50
	WAF	$0.8 \times 10^4 \pm 0.2 \times 10^4$, B	229 ± 56	172 ± 42
	Corexit	$5.0 \times 10^4 \pm 3.1 \times 10^4$, AB	n.a.[c]	n.a.
	CEWAF	$7.7 \times 10^4 \pm 2.8 \times 10^4$, A	n.a.	n.a.
Deep water	initial whole water	$2.7 \times 10^5 \pm 2.7 \times 10^3$, C	59 ± 5, B	44 ± 3, B
	whole water	$2.7 \times 10^5 \pm 2.0 \times 10^4$, C	58 ± 1, B	43 ± 10, B
	WAF	$1.6 \times 10^7 \pm 2.3 \times 10^6$, A	3719 ± 1749, A	2789 ± 1312, A
	Corexit	$8.0 \times 10^6 \pm 2.9 \times 10^6$, B	n.a.	n.a.
	CEWAF	$1.6 \times 10^6 \pm 3.1 \times 10^5$, C	n.a.	n.a.

[a] Results for surface water from Malkin et al. (2019); for deep water from Kleindienst et al. (2015b).

[b] Letters indicate results of the post-hoc analysis of treatment-specific differences (ANOVA, $p < 0.05$); rates with the same letters are indistinguishable from one another.

[c] Not available.
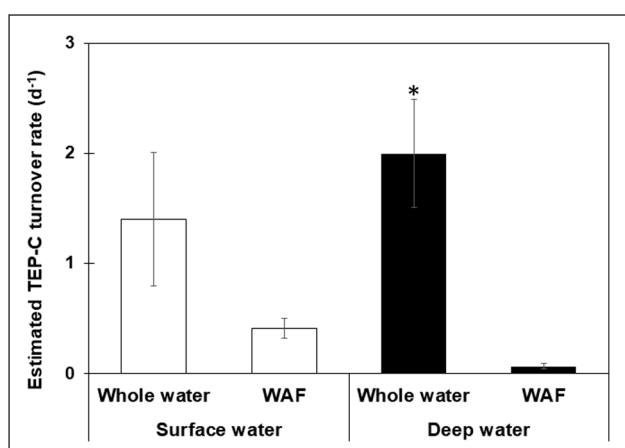
Figure 5: Estimated carbon turnover rates within the TEP-C pool. Turnover rates per day were calculated as the ratio of C remineralization rates (μg C L^{-1} d^{-1}) to TEP-C (μg C L^{-1}). See text for more details. Note that differences in the deep-water treatments (but not in the surface-water treatments) were significant (Student's t-test, $p < 0.05$). DOI: https://doi.org/10.1525/elementa.371.f5

4. Discussion

Microbial communities indigenous to the numerous oil and gas seeps in the northern Gulf of Mexico are constantly exposed to low levels of hydrocarbons. During the 2010 oil spill, however, hydrocarbon levels in the water column increased drastically, with consequences for microbial activities in the affected areas (King et al., 2015, and references therein). The application of chemical dispersants (Corexit 9500) to surface and deep waters near the spill site added another level of complexity to the system. Understanding the consequences of oil and Corexit exposure on bioremediation processes during a spill requires specific experiments like the ones described here.

As presented and discussed in more detail in Malkin et al. (2019) and Kleindienst et al. (2015b), bacteria capable of degrading hydrocarbons became persistently enriched in the surface- and deep-water amendments over the time course of the incubations. The hydrocarbon-degrading community in the surface-water WAF treatment was dominated by members of the genera *Marinobacter*, *Alcanivorax*, and to a lesser extent *Alteromonas*. *Marinobacter* and *Alcanivorax* species were also enriched in the CEWAF treatment, while the Corexit-only treatment mainly stimulated growth of *Alcanivorax* spp. The deep-water WAF amendment revealed a substantial enrichment in members of the genus *Marinobacter*, whereas the two Corexit-containing treatments (Corexit-only and CEWAF) selected for psychrophilic *Colwellia* spp.

In addition to their ability to degrade hydrocarbons, members of these genera are also known producers of EPS (Casillo et al., 2018, and references therein). For instance, *Alteromonas* isolates grown on marine broth and glucose produced complex exopolysaccharides containing structural compounds (fucose, rhamnose, glucose, galactose, mannose, galacturonic acid and glucuronic acid; Le Costaouëc et al., 2012) similar to those of the polysaccharides used in this study. *Alcanivorax* spp. grown on

alkane formed cell aggregates supported by enhanced EPS production (Sabirova et al., 2011). Analysis of EPS produced by *Marinobacter* isolates revealed high levels of carbohydrates with a broad range of structural monosaccharides (Caruso et al., 2019), including xylose (Bhaskar et al., 2005). Members of the genus *Colwellia* isolated from cold waters and sediments produced cryoprotectant EPS (Marx et al., 2009) as well as EPS enriched in deoxysugar-containing polysaccharides (Casillo et al., 2017). The latter are major components of particulate EPS and TEP (Mopper et al., 1995; Zhou et al., 1998), which also formed in our WAF amendments (**Table 4**).

For this study, we focused on the potential of heterotrophic microbial communities to degrade EPS components (polysaccharides), assuming that most of the EPS in the amended treatments were produced by primary oil degraders in response to oil and Corexit. Exopolymers produced by autotrophic organisms in the surface-water experiment possibly played a minor role, as the roller bottles were incubated in the dark. A potential priming effect of deep-water communities by sinking organic carbon, and thus a potential seasonal impact of hydrolysis patterns in deep waters, is highly unlikely as POC export fluxes in the investigation area are relatively low and decoupled from primary productivity (Giering et al., 2018).

We assumed that oil- and Corexit-induced EPS fueled activities of microbial communities not directly involved in primary oil degradation (i.e., secondary consumers; Head et al., 2006). Hydrolyis rates and patterns of the six polysaccharide substrates measured here thus include activities of non-oil degraders with broad metabolic capabilities, such as members of *Alphaproteobacteria* and *Bacteriodetes* that dominated bacterial community composition in the two experiments (Malkin et al., 2019; Kleindienst et al., 2015b). Polysaccharide hydrolysis patterns were used to infer the types and structures of polymers that microbes were capable of hydrolyzing, and by inference were likely present in our incuabtions.

4.1. Polysaccharide hydrolysis patterns in the surface-water roller bottles

Hydrolysis in the unamended surface-water treatment, which was characterized by the full spectrum of polysaccharide-hydrolyzing enzymes, was generally dominated by laminarinase and xylanase activities. This pattern agrees with our previous work on polysaccharide hydrolysis in Gulf of Mexico surface waters (Ziervogel et al., 2011; Steen et al., 2012). The ability to degrade laminarin (glucose polymer) and xylan (xylose polymer) is widespread among marine bacteria (Arnosti et al., 2011), as glucose and xylose polymers are among the most abundant components of the marine DOM pool (McCarthy et al., 1996), including microbial EPS (Bhaskar et al., 2005; Alderkamp et al., 2007; Casillo et al., 2018; Gutierrez et al., 2018; Xu et al., 2018). In contrast, low or near-zero hydrolysis of arabinogalactan (i.e., a mixed polymers of galactose and arabinose; **Table 1**), as observed in our treatments, has been reported in different marine environments (Arnosti et al., 2011), emphasizing that chemical complexity may impede enzymatic degradation of specific substrates.

Addition of WAF and Corexit-only resulted in more focused enzymatic responses compared with the unamended and CEWAF roller bottles. Lowest diversity of substrate hydrolysis was found in the WAF treatment, indicating that oil-degrading microbes exposed to undispersed oil produced a somewhat narrow range of EPS. The time courses of polysaccharide hydrolysis present further evidence for compositional differences in the respective EPS pools. While hydrolysis in the whole water, Corexit-only, and CEWAF treatments at the first sampling time (day 3) were dominated by two or three of the six substrates, substantial hydrolysis in the WAF treatment at the day-3 time point was dominated by fucoidan only (**Figure 2**). In general, the time course over which a polysaccharide was hydrolyzed in our experiments provides information about the reaction time of the microbial community to the input of a specific substrate, which could be fast if the substrate was already present in the EPS pool. Thus, the dominance of fucoidan hydrolysis in the WAF at day 3 suggests that fucoidan, or polymers with a similar chemical composition, comprised the major fraction of oil-induced EPS at the end of the WAF incubation.

The dominance of sulfated deoxysugar-containing polysaccharides, a chemical description that fits fucoidan, could also explain elevated TEP levels in the WAF relative to the unamended treatment. A previous mesocosm study with Gulf of Mexico surface waters found substantial levels of fucose in particulate EPS from phytoplankton with their associated bacterial communities exposed to oil and Corexit (Xu et al., 2018). Similar patterns emerged in our earlier study with GC600 surface waters, demonstrating good correlation between TEP, microbial oil degradation and hydrolytic enzyme activities (Ziervogel et al., 2014). These findings together with the present results underline the important role of particulate EPS/TEP in microbial oil degradation cascades in the investigation area.

An alternative explanation for the reduced enzymatic diversity and total hydrolysis rates in the WAF relative to the other surface-water treatments could be that hydrolytic potentials were reduced due to lower bacterial abundances in the presence of WAF. Bacterivorous grazers in the source water, which were not removed prior to the onset of the roller bottle experiment, may have responded to the addition of oil and Corexit in a similar way as described by Ortmann et al. (2012), who found an increase in ciliate biomass following the addition of WAF to Gulf of Mexico surface waters. In contrast, Corexit and CEWAF inhibited growth of ciliates compared to their unamended treatment.

Hydrolysis patterns in the Corexit-only treatment were very similar those in the WAF roller bottles, suggesting structural similarities within the two EPS pools. The dispersing agent Corexit is comprised of ~50% hydrocarbons (King et al., 2015) that possibly underwent biodegradation with the aid of EPS, including sulfated polysacchairdes such as fucoidan. Laboratory studies demonstrated the ability to break down hydrocarbon compounds of Corexit by oil-degrading bacteria including *Alcanivorax* isolates (Chakraborty et al., 2012), which were also present in our roller bottles.

Hydrolysis patterns in the CEWAF treatment differed from the other amended treatments. Most notably, xylan was rapidly hydrolyzed in the CEWAF, reaching overall highest hydrolysis rates at day 3 (**Figure 2**). Kamalanathan et al. (2018) also found greatly enhanced glucosidase activities in mesocosms with Gulf of Mexico waters amended with CEWAF. The pattern observed here, which was distinct from the other treatments, indicates the presence of xylose-containing polymers as part of the EPS produced by oil-degraders such as *Marinobacter* (Baskar et al., 2005) that were present in the CEWAF treatment (Malkin et al., 2019). In addition, break-down products of Corexit could have stimulated rapid xylan hydrolysis (see below).

4.2. Polysaccharide hydrolysis patterns in the deep-water roller bottles

The addition of oil and Corexit stimulated production of EPS, resulting in elevated summed hydrolysis rates in the amended compared with the unamended roller bottles (**Figure 3**). Most notably, all of our deep-water incubations showed a reduced spectrum of polysaccharide-hydrolyzing enzymes, as fucoidan and arabinogalactan remained unhydrolyzed during our time-course incubations (**Figure 4**). Using the same suite of subtrates, Steen et al. (2012) could not detect pullulan and arabinogalactan hydrolysis in deep Gulf of Mexico waters, while pulluan, arabinogalactan, and fucoidan remained unhydrolyzed in samples from deep-water hydrocarbon plumes during the DWH spill (Ziervogel and Arnosti, 2016). In the present study, the lack of fucoidan hydrolysis, in particular, indicates fundamental structural differences between the deep-water and surface-water EPS pools.

While fucoidan hydrolysis was not detectable, chondroitin sulfate hydrolysis was rapid (detectable at day 3 in WAF and Corexit-only) and substantial (overall highest rates in CEWAF at day 7) in the deep-water amendments. These differences in substrate specificities between the surface- and deep-water roller bottles may be at least in part the result of the extended incubation times of the latter (6 weeks for deep water vs. 8 days for surface water). During that time biodegradation of undispersed oil in the WAF was substantial (Kleindienst et al., 2015b), resulting in the accumulation of EPS in the form of TEP, which were orders of magnitude higher compared with the surface-water WAF, reaching levels comparable to highly productive coastal environments (e.g., Najdek et al., 2011). Elevated levels of TEP in the deep-water amendments stimulated activities of enzymes capable of degrading polymers enriched in uronic acids, such as chondroitin sulfate, and polymers enriched in glucose (laminarin and pullulan; **Figure 4**). Both glucose and uronic acids are often abundant in microbial EPS (Baskar et al., 2005), including those induced by oil and Corexit (Xu et al., 2018).

Similar to fucoidan, chondroitin is a sulfated polymer (**Table 1**); thus hydrolysis of chondroitin in the Corexit-containing roller bottles may reflect enzymatic responses to degradation byproducts of Corexit that were enriched in sulfur-containing substances, accumulating throughout the roller bottle incubation (Seidel et al., 2016). The fact that the sulfur-containing organic matter did not result in hydrolysis of fucoidan reflects structural specificities

of bacterial organic matter involved in oil and Corexit degradation.

Results from our hydrolysis time courses revealed rapid and substantial xylanase activities in the two Corexit-containing treatments, similar to the surface-water CEWAF. Our previous work also revealed rapid xylan hydrolysis in Gulf of Mexico deep-waters sampled within deep hydrocarbon plumes during the 2010 DWH spill (Ziervogel and Arnosti, 2016). Moreover, Lu et al. (2012) reported a higher presence of genes associated with the degradation of high molecular weight carbohydrates, including xylan, in deep-water plume-associated compared with non-plume associated microbial communities. Thus elevated xylan hydrolysis could be a common pattern in deep-waters containing chemically-dispersed oil, reflecting specific compounds within the pool of microbial EPS and/or degradation byproducts of Corexit.

5. Conclusions

Our results of polysaccharide hydrolysis provide insights into potential enzymatic responses of heterotrophic microbial communities to organic matter that formed during oil degradation, including EPS that serves as biosurfactants for oil-degrading bacterial populations. Surface- and deep-water communities showed distinct patterns of polysaccharide hydrolysis. In addition to compositional differences within the respective EPS pools, variations in oil-degrading bacterial populations may have affected hydrolytic potentials in the surface- and deep-water roller bottles. The most notable difference was the enrichment of the genus *Colwellia* in the Corexit-containing deep-water roller bottles (Kleindienst et al., 2015b). Members of the genus *Colwellia* were not detectable in the surface-water amendments (Malkin et al., 2019) but were found during the DWH spill in the deep-water hydrocarbon plumes containing particulate EPS (Bælum et al., 2012). In addition to EPS production and hydrocarbon degradation, *Colwellia* spp. are capable of degrading Corexit components (e.g., Chakraborty et al., 2012), a trait that could explain at least in part the observed differences in hydrolysis patterns between the Corexit-containing surface-water and deep-water roller bottles.

Other factors that may have affected the observed differences in hydrolysis patterns between the two roller bottle experiments include differences in roller bottle incubation times as well as the levels of oil and Corexit added to the source water (**Table S1**). Moreover activities of surface-water communities were limited by inorganic nutrients, as discussed in Malkin et al. (2019), and subject to eukaryotic grazers with different outcomes in the presence and absence of Corexit, as discussed above. Despite these factors that complicate a direct comparison of the two experiments, our results indicate an overall enhancement of polysaccharide hydrolysis in deep waters whereas degradation patterns in surface waters may be more complex.

Our model calculation of TEP-C turnover helps to interpret hydrolysis patterns with respect to the fate of EPS in oil-contaminated waters (**Figure 5**). Lower calculated turnover rates of TEP-C in the presence of WAF indicate that only a small fraction of oil-induced TEP-C is available for processing by heterotrophic communities throughout the water column. Particulate EPS may thus accumulate in the presence of oil and Corexit as demonstrated by other recent laboratory experiments with Gulf of Mexico waters (e.g., Xu et al., 2018). High levels of TEP in oil-contaminated waters may then enhance the 'stickiness' of particulate matter, accelerating particle formation and the aggregation of marine oil snow (Passow, 2016) with consequences for the fate of spilled oil in the ocean.

Competing interests

The authors have no competing interests to declare.

Author contributions

· Contributed to conception and design: KZ, SBJ, SK, SYM
· Contributed to acquisition of data: KZ, SK, SYM, UP, CA
· Contributed to analysis and interpretation of data: KZ, SK, SYM, UP, ADS, CA
· Wrote the manuscript: KZ, CA
· Approved the submitted version for publication: all

References

Alderkamp, C, van Rijssel, M and **Bolhuis, H.** 2007. Characterization of marine bacteria and the activity of their enzyme systems involved in degradation of the algal storage glucan laminarin. *FEMS Microbiol Ecol* **59**: 108–117. DOI: https://doi.org/10.1111/j.1574-6941.2006.00219.x

Arnosti, C. 1996. A new method for measuring polysaccharide hydrolysis rates in marine environments. *Org Geochem* **25**: 105–115. DOI: https://doi.org/10.1016/S0146-6380(96)00112-X

Arnosti, C. 2003. Fluorescent derivatization of polysaccharides and carbohydrate-containing biopolymers for measurement of enzyme activities in complex media. *J Chromatogr B* **793**: 181–191. DOI: https://doi.org/10.1016/S1570-0232(03)00375-1

Arnosti, C, Steen, AD, Ziervogel, K, Ghobrial, S and **Jeffrey, WH.** 2011. Latitudinal gradients in degradation of marine dissolved organic carbon. *PLOS ONE* **6**: e28900. DOI: https://doi.org/10.1371/journal.pone.0028900

Arnosti, C, Ziervogel, K, Yang, T and **Teske, A.** 2016. Oil-derived marine aggregates – hot spots of polysaccharide degradation by specialized bacterial communities. *Deep Sea Res II*. DOI: https://doi.org/10.1016/j.dsr2.2014.12.008

Bælum, J, Borglin, S, Chakraborty, R, Fortney, JL, Lamendella, R, Mason, OU, Auer, M, Zemla, M, Bill, M, Conrad, ME, Malfatti, SA, Tringe, SG, Holman, H-Y, Hazen, TC and **Jansson, JK.** 2012. Deep-sea bacteria enriched by oil and dispersant from the Deepwater Horizon spill. *Environ Microbiol* **14**: 2405–2416. DOI: https://doi.org/10.1111/j.1462-2920.2012.02780.x

Bauer, M, Kube, M, Teeling, H, Richter, M, Lombardot, T, Allers, E, Würdemann, CA, Quast, C, Kuhl, H, Knaust, F, Woebken, D, Bischof, K, Mussmann, M, Choudhuri, JV, Meyer, F, Reinhardt, R, Amann, RI and **Glöckner, FO.** 2006. Whole genome analysis of the marine Bacteroidetes 'Gramella forsetii' reveals adaptations to degradation of polymeric organic matter. *Environ Microbiol* **8**: 2201–2213. DOI: https://doi.org/10.1111/j.1462-2920.2006.01152.x

Bhaskar, PV, Grossart, HP, Bhosle, NB and **Simon, M.** 2005. Production of macroaggregates from dissolved exopolymeric substances (EPS) of bacterial and diatom origin. *FEMS Microbiol Ecol* **53**: 255–264. DOI: https://doi.org/10.1016/j.femsec.2004.12.013

Caruso, C, Rizzo, C, Mangano, S, Poli, A, Di Donato, P, Nicolaus, B, Finore, I, Di Marco, G, Michaud, L and **Lo Giudice, A.** 2019. Isolation, characterization and optimization of EPSs produced by a cold-adapted *Marinobacter* isolate from Antarctic seawater. *Antarct Sci* **31**(2): 69–79. DOI: https://doi.org/10.1017/S0954102018000482

Casillo, A, Lanzetta, R, Parrilli, M and **Corsaro, MM.** 2018. Exopolysaccharides from marine and marine extremophilic bacteria: structures, properties, ecological roles and applications. *Mar Drugs* **16**: 69. DOI: https://doi.org/10.3390/md16020069

Casillo, A, Ståhle, J, Parrilli, E, Sannino, F, Mitchell, DE, Pieretti, G, Gibson, MI, Marino, G, Lanzetta, R, Parrilli, M, Widmalm, G, Tutino, ML and **Cosaro, MM.** 2017. Structural characterization of an all-aminosugar-containing capsular polysaccharide from *Colwellia psychrerythraea* 34H. *A Van Leeuw* **110**: 1377–1387. DOI: https://doi.org/10.1007/s10482-017-0834-6

Chakraborty, R, Borglin, SE, Dubinsky, EA, Andersen, GL and **Hazen, TC.** 2012. Microbial response to the MC-252 oil and Corexit 9500 in the Gulf of Mexico. *Front Microbiol.* DOI: https://doi.org/10.3389/fmicb.2012.00357

Chanton, J, Zhao, T, Rosenheim, BE, Joye, S, Bosman, S, Brunner, C, Yeager, KM, Diercks, AR and **Hollander, D.** 2015. Using natural abundance radiocarbon to trace the flux of petrocarbon to the seafloor following the Deepwater Horizon oil spill. *Environ Sci Technol* **49**: 847–854. DOI: https://doi.org/10.1021/es5046524

Diercks, AR, Highsmith, RC, Asper, VL, Joung, D, Zhou, Z, Guo, L, Shiller, AM, Joye, SB, Teske, A, Guinasso, N, Wade, TL and **Lohrenz, SE.** 2010. Characterization of subsurface polycyclic aromatic hydrocarbons at the Deepwater Horizon site. *Geophys Res Lett* **37**. DOI: https://doi.org/10.1029/2010GL045046

Edwards, BR, Reddy, CM, Camilli, R, Carmichael, CA, Longnecker, K and **van Mooy, B.** 2011. Rapid microbial respiration of oil from the Deepwater Horizon spill in offshore surface-waters of the Gulf of Mexico. *Environ Res Lett* **6**: 035301. DOI: https://doi.org/10.1088/1748-9326/6/3/035301

Engel, A and **Passow, U.** 2001. Carbon and nitrogen content of transparent exopolymer particles (TEP) in relation to their Alcian Blue adsorption. *Mar Ecol-Prog Ser* **219**: 1–10. DOI: https://doi.org/10.3354/meps219001

Giering, SLC, Yan, B, Sweet, J, Asper, V, Diercks, A, Chanton, JP, Pitiranggon, M and **Passow, U.** 2018. The ecosystem baseline for particle flux in the Northern Gulf of Mexico. *Elem Sci Anth* **6**(1). DOI: https://doi.org/10.1525/elementa.264

Glöckner, FO, Kube, M, Bauer, M, Teeling, H, Lombardot, T, Ludwig, W, Gade, D, Beck, A, Borzym, K, Heitmann, K, Rabus, R, Schlesner, H, Amann, R and **Reinhardt, R.** 2003. Complete genome sequence of the marine planctomycete *Pirellula* sp. strain 1. *Proc Natl Acad Sci USA* **100**: 8298–8303. DOI: https://doi.org/10.1073/pnas.1431443100

Gutierrez, T, Berry, D, Yang, T, Mishamandani, S, McKay, L, Teske, A and **Aitken, MD.** 2013. Role of bacterial exopolysaccharides (EPS) in the fate of the oil released during the Deepwater Horizon oil apill. *PLOS ONE* **8**: e67717. DOI: https://doi.org/10.1371/journal.pone.0067717

Gutierrez, T, Morris, G, Ellis, D, Bowler, B, Jones, M, Salek, K, Mulloy, B and **Teske, A.** 2018. Hydrocarbon-degradation and MOS-formation capabilities of the dominant bacteria enriched in sea surface oil slicks during the Deepwater Horizon oil spill. *Mar Pollut Bull* **135**: 205–215. DOI: https://doi.org/10.1016/j.marpolbul.2018.07.027

Hazen, TC, Dubinsky, EA, DeSantis, TZ, Andersen, GL, Piceno, YM, Singh, N, Jansson, JK, Probst, A, Borglin, SE, Fortney, JL, Stringfellow, WT, Bill, M, Conrad, ME, Tom, LM, Chavarria, KL, Alusi, TR, Lamendella, R, Joyner, DC, Spier, C, Bælum, J, Auer, M, Zemla, ML, Chakraborty, R, Sonnenthal, EL, D'Haeseleer, P, Holman, H-YN, Osman, S, Lu,

Z, Nostrand, JDV, Deng, Y, Zhou, J and **Mason, OU.** 2010. Deep-sea oil plume enriches indigenous oil-degrading bacteria. *Science* **330**: 204–208. DOI: https://doi.org/10.1126/science.1195979

Head, IM, Jones, DM and **Röling, WFM.** 2006. Marine microorganisms make a meal of oil. *Nat Rev Microbiol* **4**: 173–182. DOI: https://doi.org/10.1038/nrmicro1348

Joye, SB, Bowles, MW, Samarkin, VA, Hunter, KS and **Niemann, H.** 2010. Biogeochemical signatures and microbial activity of different cold-seep habitats along the Gulf of Mexico deep slope. *Deep Sea Res II* **57**: 1990–2001. DOI: https://doi.org/10.1016/j.dsr2.2010.06.001

Kamalanathan, M, Xu, C, Schwehr, K, Bretherton, L, Beaver, M, Doyle, SM, Genzer, J, Hillhouse, J, Sylvan, JB, Santschi, P and **Quigg, A.** 2018. Extracellular enzyme activity profile in a chemically enhanced water accommodated fraction of surrogate oil: Toward understanding microbial activities after the Deepwater Horizon Oil Spill. *Front Microbiol* **9**. DOI: https://doi.org/10.3389/fmicb.2018.00798

Kleindienst, S, Grim, S, Sogin, M, Bracco, A, Crespo-Medina, M and **Joye, SB.** 2016. Diverse, rare microbial taxa responded to the *Deepwater Horizon* deep-sea hydrocarbon plume. *ISME J* **10**: 400–415. DOI: https://doi.org/10.1038/ismej.2015.121

Kleindienst, S, Paul, JH and **Joye, SB.** 2015a. Using dispersants after oil spills: impacts on the composition and activity of microbial communities. *Nat Rev Microbiol* **13**: 388–396. DOI: https://doi.org/10.1038/nrmicro3452

Kleindienst, S, Seidel, M, Ziervogel, K, Grim, S, Loftis, K, Harrison, S, Malkin, SY, Perkins, MJ, Field, J, Sogin, ML, Dittmar, T, Passow, U, Medeiros, PM and **Joye, SB.** 2015b. Chemical dispersants can suppress the activity of natural oil-degrading microorganisms. *PNAS* **112**: 14900. DOI: https://doi.org/10.1073/pnas.1507380112

Kujawinski, L, Sole, MCK, Valentine, DL, Boysen, AK, Longnecker, K and **Redmond, MC.** 2011. Fate of dispersants associated with the Deepwater Horizon oil spill. *Environ Sci Technol* **45**: 1298–1306. DOI: https://doi.org/10.1021/es103838p

Le Costaouëc, T, Cérantola, S, Ropartz, D, Ratiskol, J, Sinquin, C, Colliec-Jouault, S and **Boisset, C.** 2012. Structural data on a bacterial exopolysaccharide produced by a deep-sea *Alteromonas macleodii* strain. *Carbohydr Polym* **90**: 49–59. DOI: https://doi.org/10.1016/j.carbpol.2012.04.059

MacDonald, IR, Garcia-Pineda, O, Beet, A, Asl, SD, Feng, L, Graettinger, G, French-McCay, D, Holmes, J, Hu, C, Huffer, F, Leifer, I, Muller-Karger, F, Solow, A, Silva, M and **Swayze, G.** 2015. Natural and unnatural oil slicks in the Gulf of Mexico. *J Geophys Res Oceans* **120**: 8364–8380. DOI: https://doi.org/10.1002/2015JC011062

Malkin, SY, Saxton, M, Harrison, S, Battles, J, Sweet, J, Passow, U and **Joye, SB.** 2019. Remarkable variability in microbial hydrocarbon oxidation rates in surface waters in the Gulf of Mexico. *Elem Sci Anth.* (submitted).

Marx, JG, Carpenter, SD and **Deming, JW.** 2009. Production of cryoprotectant extracellular polysaccharide substances (EPS) by the marine psychrophilic bacterium *Colwellia psychrerythraea* strain 34H under extreme conditions. *Can J Microbiol* **55**: 63–72. DOI: https://doi.org/10.1139/W08-130

Mopper, K, Zhou, JA, Ramana, KS, Passow, U, Dam, HG and **Drapeau, DT.** 1995. The role of surface-active carbohydrates in the flocculation of a diatom bloom in a mesocosm. *Deep Sea Res II* **42**: 47–73. DOI: https://doi.org/10.1016/0967-0645(95)00004-A

Najdek, M, Blažina, M, Fuks, D, Ivančić, I and **Šilović, T.** 2011. Intrusion of high-salinity water causes accumulation of transparent exopolymer particles (TEP) in the northern Adriatic Sea. *Aquat Microb Ecol* **63**: 69–74. DOI: https://doi.org/10.3354/ame01476

Oksanen, J, Blanchet, FG, Friendly, M, Kindt, R, Legendre, P, McGlinn, D, Minchin, PR, O'Hara, RB, Simpson, GL, Solymos, P, Stevens, MHH, Szoecs, E and **Wagner, H.** 2017. vegan: Community Ecology Package.

Ortmann, AC, Anders, J, Shelton, N, Gong, L, Moss, AG and **Condon, RH.** 2012. Dispersed oil disrupts microbial pathways in pelagic food webs. *PLOS ONE* **7**: e42548. DOI: https://doi.org/10.1371/journal.pone.0042548

Overton, E, Wade, T, Radovic, J, Meyer, B, Miles, MS and **Larter, S.** 2016. Chemical composition of macondo and other crude oils and compositional alterations during oil spills. *Oceanography* **29**: 50–63. DOI: https://doi.org/10.5670/oceanog.2016.62

Passow, U. 2002. Transparent exopolymer particles (TEP) in aquatic environments. *Prog Oceanogr* **55**: 287–333. DOI: https://doi.org/10.1016/S0079-6611(02)00138-6

Passow, U. 2016. Formation of rapidly-sinking, oil-associated marine snow. *Deep Sea Res II* **129**: 232–240. DOI: https://doi.org/10.1016/j.dsr2.2014.10.001

Passow, U and **Alldredge, AL.** 1995. A dye-binding assay for the spectrophotometric measurement of transparent exopolymer particles (TEP). *Limnol Oceanogr* **40**: 1326–1335. DOI: https://doi.org/10.4319/lo.1995.40.7.1326

Passow, U, Sweet, J and **Quigg, A.** 2017. How the dispersant Corexit impacts the formation of sinking marine oil snow. *Mar Pollut Bull* **125**: 139–145. DOI: https://doi.org/10.1016/j.marpolbul.2017.08.015

Passow, U and **Ziervogel, K.** 2016. Marine snow sedimented oil released during the Deepwater Horizon spill. *Oceanography* **29**: 118–125. DOI: https://doi.org/10.5670/oceanog.2016.76

Passow, U, Ziervogel, K, Asper, V and **Diercks, A.** 2012. Marine snow formation in the aftermath of the Deepwater Horizon oil spill in the Gulf of Mexico. *Environ Res Lett* **7**: 035301. DOI: https://doi.org/10.1088/1748-9326/7/3/035301

Quigg, A, Passow, U, Chin, W-C, Xu, C, Doyle, S, Bretherton, L, Kamalanathan, M, Williams, AK, Sylvan, JB, Finkel, ZV, Knap, AH, Schwehr, KA, Zhang, S, Sun, L, Wade, TL, Obeid, W, Hatcher, PG and **Santschi, PH.** 2016. The role of microbial exopolymers in determining the fate of oil and chemical dispersants in the ocean. *Limnol Oceanogr Lett* **1**: 3–26. DOI: https://doi.org/10.1002/lol2.10030

Redmond, MC and **Valentine, DL.** 2011. Natural gas and temperature structured a microbial community response to the Deepwater Horizon oil spill. *Proc Natl Acad Sci USA* **109**: 20,292–20,297. DOI: https://doi.org/10.1073/pnas.1108756108

Sabirova, JS, Becker, A, Lünsdorf, H, Nicaud, JM, Timmis, KM and **Golyshin, PN.** 2011. Transcriptional profiling of the marine oil-degrading bacterium *Alcanivorax borkumensis* during growth on *n*-alkanes. *FEMS Microbiol Lett* **319**: 160–168. DOI: https://doi.org/10.1111/j.1574-6968.2011.02279.x

Seidel, M, Kleindienst, S, Dittmar, T, Joye, SB and **Medeiros, PM.** 2016. Biodegradation of crude oil and dispersants in deep seawater from the Gulf of Mexico: Insights from ultra-high resolution mass spectrometry. *Deep Sea Res II* **129**: 108–118. DOI: https://doi.org/10.1016/j.dsr2.2015.05.012

Steen, AD, Ziervogel, K, Ghobrial, S and **Arnosti, C.** 2012. Functional variation among polysaccharide-hydrolyzing microbial communities in the Gulf of Mexico. *Mar Chem* **138**: 13–20. DOI: https://doi.org/10.1016/j.marchem.2012.06.001

Techtmann, SM, Zhuang, M, Campo, P, Holder, E, Elk, M, Hazen, TC, Conmy, R and **Santo Domingo, JW.** 2017. Corexit 9500 enhances oil biodegradation and changes active bacterial community structure of oil-enriched microcosms. *Appl Environ Microbiol* **83**: e03462-16. DOI: https://doi.org/10.1128/AEM.03462-16

Valentine, DL, Kessler, JD, Redmond, MC, Mendes, SD, Heintz, MB, Farwell, C, Hu, L, Kinnaman, FS, Yvon-Lewis, S, Du, M, Chan, EW, Tigreros, FG and **Villanueva, CJ.** 2010. Propane respiration jump-starts microbial response to a deep oil spill. *Science* **330**: 208–211. DOI: https://doi.org/10.1126/science.1196830

van Eenennaam, JS, Wei, Y, Grolle, KCF, Foekema, EM and **Murk, AJ.** 2016. Oil spill dispersants induce formation of marine snow by phytoplankton-associated bacteria. *Mar Pollut Bull* **104**: 294–302. DOI: https://doi.org/10.1016/j.marpolbul.2016.01.005

Wade, TL, Morales-McDevitt, M, Bera, G, Shi, D, Sweet, S, Wang, B, Gold-Bouchot, G, Quigg, A and **Knap, AH.** 2017. A method for the production of large volumes of WAF and CEWAF for dosing mesocosms to understand marine oil snow formation. *Heliyon* **3**: e00419. DOI: https://doi.org/10.1016/j.heliyon.2017.e00419

Weiner, RM, Taylor II, LE, Henrissat, B, Hauser, L, Land, M, Coutinho, PM, Rancurel, C, Saunders, EH, Longmire, AG, Zhang, H, Bayer, EA, Gilbert, HJ, Larimer, F, Zhulin, IB, Ekborg, NA, Lamed, R, Richardson, PM, Borovok, I and **Hutcheson, S.** 2008. Complete genome sequence of the complex carbohydrate-degrading marine bacterium, *Saccharophagus degradans* strain 2-40T. *PLOS Genet* **5**: e1000087. DOI: https://doi.org/10.1371/journal.pgen.1000087

Xu, C, Zhang, S, Beaver, M, Lin, P, Sun, L, Doyle, SM, Sylvan, JB, Wozniak, A, Hatcher, PG, Kaiser, K, Yan, G, Schwehr, KA, Lin, Y, Wade, TL, Chin, W-C, Chiu, M-H, Quigg, A and **Santschi, PH.** 2018. The role of microbially-mediated exopolymeric substances (EPS) in regulating Macondo oil transport in a mesocosm experiment. *Mar Chem* **206**: 52–61. DOI: https://doi.org/10.1016/j.marchem.2018.09.005

Yang, T, Nigro, LM, Gutierrez, T, D'Ambrosio, L, Joye, SB, Highsmith, R and **Teske, A.** 2016. Pulsed blooms and persistent oil-degrading bacterial populations in the water column during and after the Deepwater Horizon blowout. *Deep Sea Res II* **129**: 282–291. DOI: https://doi.org/10.1016/j.dsr2.2014.01.014

Zhou, J, Mopper, K and **Passow, U.** 1998. The role of surface-active carbohydrates in the formation of transparent exopolymer particles by bubble adsorption of seawater. *Limnol Oceanogr* **43**: 1860–1871. DOI: https://doi.org/10.4319/lo.1998.43.8.1860

Ziervogel, K and **Arnosti, C.** 2016. Enhanced protein and carbohydrate hydrolyses in plume-associated deepwaters initially sampled during the early stages of the Deepwater Horizon oil spill. *Deep Sea Res II* **129**: 368–373. DOI: https://doi.org/10.1016/j.dsr2.2013.09.003

Ziervogel, K, D'souza, N, Sweet, J, Yan, B and **Passow, U.** 2014. Natural oil slicks fuel surface-water microbial activities in the northern Gulf of Mexico. *Front Microbiol* **5**. DOI: https://doi.org/10.3389/fmicb.2014.00188

Ziervogel, K, McKay, L, Rhodes, B, Osburn, CL, Dickson-Brown, J, Arnosti, C and **Teske, A.** 2012. Microbial activities and dissolved organic matter dynamics in oil-contaminated surface seawater from the Deepwater Horizon oil spill site. *PLOS ONE* **7**: e34816. DOI: https://doi.org/10.1371/journal.pone.0034816

Ziervogel, K, Steen, AD and **Arnosti, C.** 2011. Changes in the spectrum and rates of extracellular enzyme activities in seawater following aggregate formation. *Biogeosci* **7**: 1007–1015. DOI: https://doi.org/10.5194/bg-7-1007-2010